Kinetics and Catalysis, Vol. 44, No. 1, 2003, pp. 28–39. Translated from Kinetika i Kataliz, Vol. 44, No. 1, 2003, pp. 35–46.

Kinetics of Detonation Initiation in the Supersonic Flow of the $H_2 + O_2$ (Air) Mixture in O_2 Molecule Excitation by Resonance Laser Radiation

A. M. Starik and N. S. Titova

Baranov Central Institute of Aviation Motors, Moscow, Russia

Received March 1, 2002

Abstract—The possibility of initiating detonation in the supersonic flow of the $H_2 + O_2$ (air) mixture behind the front of the inclined shock wave by O_2 molecule excitation to the $O_2(a^1\Delta_g)$ and $O_2(b^1\Sigma_g^+)$ states by laser radiation with a wavelength λ_I = 1.268 μm and 762 nm is considered. Resonance laser radiation intensifies chain combustion due to the formation of new pathways for generating active atoms $O^\cdot$ and $H^\cdot$ and radicals $\dot{O}H$ and has a substantially nonthermal character. Even at low (~3 kJ/cm^2) energies of radiation with λ_I = 762 nm applied to the gas, detonation combustion can occur even at a distance of 1 m from the front at the gas temperature as high as 600 K.

INTRODUCTION

The possibility of efficient combustion and detonation control using various physical effects has been discussed for several decades. As early as in the early 1970s, Jaggers and von Engel [1] attempted to influence combustion with an electric field. At the same time, research began into the plasma-chemical methods of affecting flames [2–4]. However, considerable progress has only been achieved in this field recently. This is primarily due to the rapid development of physicochemical kinetics and studies of nonequilibrium processes involving ions and excited atoms and molecules. At present, there are several areas of research into the intensification of combustion processes. These include the initiation of the ionic–molecular and ionic–atomic reactions under the action of electric discharge on the reaction mixture [4, 5], the formation of active atoms and radicals in the mixture during photodissociation on exposure to ultraviolet and ionizing irradiation [3, 6], the ignition of the combustible mixture on its heating by laser radiation or upon laser breakdown [7–9], and the activation of the reaction systems by the excitation of the internal degrees of freedom of molecules [10–13].

At present, the most promising (from the standpoint of affecting the initiation of combustion and detonation) and the least energy-consuming method is the selective excitation of the vibrational and electronic degrees of freedom of molecules. Indeed, the excitation of N_2 molecules in the lower vibrational state $N_2(v = 1)$ requires an energy of 0.29 eV, whereas the excitation of the O_2 molecule in the lower electronic state $O_2(a^1\Delta_g)$ needs ~0.98 eV. At the same time, the formation of atoms by O_2 molecule photodissociation or by dissociation with the electron shock requires 5.1 eV per molecule, whereas the formation of O^+, O_2^+, and N^+ ions needs more than 12 eV.

Earlier [14], we found that the preliminary excitation of the vibrational degrees of freedom of H_2 and N_2 molecules can cause noticeable acceleration of chain reactions and the initiation of the detonation combustion of the H_2 + air mixture in the supersonic flow even behind a weak inclined shock wave [14]. We also showed [15] that the excitation of molecular oxygen from the ground $X^3\Sigma_g^-$ state in the first electronically excited state $a^1\Delta_g$ can strongly affect the kinetics of the processes in the $H_2 + O_2$ mixture and decrease both the self-ignition temperature and the induction period during combustion in the supersonic flow initiated by the shock wave. These effects are due to a decrease in the barrier of the endoergic reactions involving the excited $O_2(a^1\Delta_g)$ molecules compared to the reactions of nonexcited O_2 molecules. A still more pronounced effect might be expected upon the excitation of the O_2 molecules to the second electronically excited state $b^1\Sigma_g^+$, because the $O_2(b^1\Sigma_g^+)$ molecules must be more active in overcoming the activation barrier than $O_2(a^1\Delta_g)$. The excitation of the O_2 molecules to the $a^1\Delta_g$ and $b^1\Sigma_g^+$ states may be carried out by laser irradiation with a wavelength λ_I = 1.268 μm and 762 nm, respectively [16]. Note that, in contrast to the electric discharge, this

0023-1584/03/4401-0028$25.00

excitation can easily be organized in a supersonic flow as well.

The aim of this work was to analyze the possibility of accelerating the initiation of combustion and detonation in a supersonic flow behind the inclined shock wave in O_2 molecule excitation by resonance laser radiation.

KINETIC MODEL

Even in the absence of the electronically excited O_2 molecules, it is necessary to use a rather branched kinetic scheme containing 29 reversible reactions involving $H^{\cdot}$, $O^{\cdot}$, $\dot{O}H$, H_2O, H_2, O_2, $H\dot{O}_2$, H_2O_2, and O_3 to describe the ignition of a simple $H_2 + O_2$ mixture over a wide range of initial temperatures and pressures [15, 17]. If excited $O_2(a^1\Delta_g)$ and $O_2(b^1\Sigma_g^+)$ molecules are present in the reaction mixture, the scheme should contain additional reactions also involving $O(^1D)$ atoms formed by the electron–electron exchange processes [16]. The table presents reactions involving both excited and nonexcited species included in this model, as well as the coefficients used to calculate the rate constants of the direct and reverse reactions $k_{+(-)q}(T)$ by the equation $k_q(T) = A_q T^{n_q} \exp(-E_{a,q}/kT)$, where T is the gas temperature, $E_{a,q}$ is the activation energy of the qth reaction, A_q is the Arrhenius coefficient, and k is the Boltzmann constant.

Let us consider the determination of the rate constants of the reactions involving the excited $O_2(a^1\Delta_g)$ and $O_2(b^1\Sigma_g^+)$ molecules and $O(^1D)$ atoms in more detail. The excitation of the vibrational and electronic degrees of freedom of the reacting molecules causes a decrease in the barriers of endoergic reactions [18]. The rate constant for such a reaction at $E_e < E_{a,q}^0$ (where E_e is the energy of the excited state of the reacting molecule and $E_{a,q}^0$ is the activation energy of the reaction when the given molecule is nonexcited) may be described in the usual form:

$$k_{e,q}(T) = A_q T^{n_q} \exp(-E_{a,q}^e/kT). \quad (1)$$

Here, $E_{a,q}^e$ is the activation energy of the reaction involving the excited molecule (atom).

Let us consider how the E_a^e value can be determined for the exchange reaction

$$AB(e) + C = A + BC,$$

where AB(e) is the molecule excited in some e electron state. The potential energy surface for the direct reaction can be written in a rather simple form:

$$U_1 = \Delta H + E_a^0 \exp(r/r_1),$$

where ΔH is the enthalpy of the reaction, E_a^0 is the activation energy for the direct reaction when the AB molecule is nonexcited.

In this case, the potential energy surface for the reverse reaction is

$$U_2 = (\Delta H + E_a^0)\exp(-r/r_2).$$

Here, r_1 and r_2 are the radii of the action of the exchange forces for the reactants and products, respectively. The potential energy surface for the reaction involving a molecule that is in the electonically excited state with the energy E_e is somewhat higher than that for the reaction involving the nonexcited molecule. In this case,

$$U_1^e = \Delta H + E_e + E_a^0 \exp(r/r_1).$$

As for the processes of the vibrationally excited molecules [18], we assumed here that the shape of the potential surface for the reactions involving electronically excited molecules $O_2(a^1\Delta_g)$ and $O_2(b^1\Sigma_g^+)$, as well as $O(^1D)$ atoms, U_1^e, coincides with that U_1 for the molecules present in their ground electronic state. Note that this assumption is not true in the general case.

At the intersection point, $U_1^e = U_2$. Assuming that $r_1 = r_2$ [18], we easily derive the following equation for E_a^e:

$$E_a^e = \frac{1}{2}\left(\sqrt{(\Delta H + E_e)^2 + 4E_a^0(\Delta H + E_a^0)} - (\Delta H + E_e)\right). \quad (2)$$

Note that a similar procedure was used earlier [19] to determine the activation energy for the reactions involving vibrationally excited molecules.

Using Eqs. (1) and (2), we determined the rate constants for direct (4), (5), (16), (17), (27), (28), (32), (33), (46), and (47) and reverse reactions (41), (42), (52), (53), (55), and (56) (see table). However, this method is inapplicable to calculating the rate constants for the reactions with zero activation barriers ($E_{a,q} \approx 0$) and the reactions involving excited $O_2(b^1\Sigma_g^+)$ molecules, for which the activation energy is comparable with the energy of the excited state $b^1\Sigma_g^+$ ($E_e = 1.64$ eV). The first class includes reactions forming molecular oxygen in different electron states ($X^3\Sigma_g^-$, $a^1\Delta_g$, and $b^1\Sigma_g^+$), and the second class contains the chain propagation reactions ($H^{\cdot} + O_2(b^1\Sigma_g^+) = \dot{O}H + O^{\cdot}$ and $H_2 + O_2(b^1\Sigma_g^+) = H\dot{O}_2 + H^{\cdot}$).

The rate constants for the reactions without barriers involving electronically excited molecules were calculated by a procedure described in [20]. This procedure implies that, for the reactions resulting in molecular

Reactions included in the kinetic scheme and coefficients for calculating the rate constants $k_q(T) = A_q T^{n_q} \exp(-E_{a,q}/kT)$

No.	Reaction	k_{+q} $(cm^3/mol)^{m-1}$ s^{-1}			k_{-q} $(cm^3/mol)^{m-1}$ s^{-1}		
		A_q	n_q	$E_{a,q}/k$, K	A_q	n_q	$E_{a,q}/k$, K
1	$H_2O + M = \dot{O}H + H^{\bullet} + M$	1×10^{24}	–2.2	59000	2.2×10^{22}	–2	0
2	$H_2 + M = 2H^{\bullet} + M$	2.2×10^{14}	0	48300	9×10^{17}	–1	0
3	$O_2(X\,^3\Sigma_g^-) + M = {}^{\bullet}O(^3P) + {}^{\bullet}O(^3P) + M$	5.4×10^{18}	–1	59400	6×10^{13}	0	–900
4	$O_2(a^1\Delta_g) + M = {}^{\bullet}O(^3P) + {}^{\bullet}O(^3P) + M$	5.4×10^{18}	–1	48008	–	–	–
5	$O_2(b\,^1\Sigma_g^+) + M = {}^{\bullet}O(^3P) + {}^{\bullet}O(^3P) + M$	5.4×10^{18}	–1	40415	–	–	–
6	$\dot{O}H + M = {}^{\bullet}O(^3P) + H^{\bullet} + M$	8.5×10^{18}	–1	50830	7.1×10^{18}	–1	0
7	$H_2 + {}^{\bullet}O(^3P) = \dot{O}H + H^{\bullet}$	1.8×10^{10}	1	4480	8.3×10^{9}	1	3500
8	$H_2 + {}^{\bullet}O(^1D) = \dot{O}H + H^{\bullet}$	6.27×10^{13}	0	0	–	–	–
9	$O_2(X\,^3\Sigma_g^-) + H^{\bullet} = \dot{O}H + {}^{\bullet}O(^3P)$	2.2×10^{14}	0	8455	1.3×10^{13}	0	350
10	$O_2(a^1\Delta_g) + H^{\bullet} = \dot{O}H + {}^{\bullet}O(^3P)$	1.1×10^{14}	0	3188	5.8×10^{12}	0	6224
11	$O_2(b\,^1\Sigma_g^+) + H^{\bullet} = \dot{O}H + {}^{\bullet}O(^3P)$	1.1×10^{14}	0	1620	–	–	–
12	$H_2O + {}^{\bullet}O(^3P) = 2\dot{O}H$	5.8×10^{13}	0	9059	5.3×10^{12}	0	503
13	$H_2O + {}^{\bullet}O(^1D) = 2\dot{O}H$	1.32×10^{14}	0	0	–	–	–
14	$H_2O + H^{\bullet} = \dot{O}H + H_2$	8.4×10^{13}	0	10116	2×10^{13}	0	2600
15	$H_2 + O_2(X\,^3\Sigma_g^-) = 2\dot{O}H$	1.7×10^{15}	0	24200	1.7×10^{13}	0	24100
16	$H_2 + O_2(a^1\Delta_g) = 2\dot{O}H$	1.7×10^{15}	0	17906	–	–	–
17	$H_2 + O_2(b\,^1\Sigma_g^+) = 2\dot{O}H$	1.7×10^{15}	0	14657	–	–	–
18	$HO_2^{\bullet} + M = O_2(X\,^3\Sigma_g^-) + H^{\bullet} + M$	$q_X \times 2.1 \times 10^{15}$	0	23000	1.5×10^{15}	0	–500
19	$HO_2^{\bullet} + M = O_2(a^1\Delta_g) + H^{\bullet} + M$	$q_a \times 2.1 \times 10^{15}$	0	23000	1.5×10^{15}	0	–500
20	$HO_2^{\bullet} + M = O_2(b\,^1\Sigma_g^+) + H^{\bullet} + M$	$q_b \times 2.1 \times 10^{15}$	0	23000	1.5×10^{15}	0	–500
21	$H_2 + O_2(X\,^3\Sigma_g^-) = H^{\bullet} + HO_2^{\bullet}$	1.9×10^{13}	0	24100	1.3×10^{13}	0	0
22	$H_2 + O_2(a^1\Delta_g) = H^{\bullet} + HO_2^{\bullet}$	2.1×10^{13}	0	18216	6×10^{12}	0	1518
23	$H_2 + O_2(b\,^1\Sigma_g^+) = H^{\bullet} + HO_2^{\bullet}$	2.1×10^{13}	0	11508	–	–	–
24	$H_2O + {}^{\bullet}O(^3P) = H^{\bullet} + HO_2^{\bullet}$	4.76×10^{11}	0.372	28743	1×10^{13}	0	540
25	$H_2O + {}^{\bullet}O(^1D) = H_2 + O_2(X\,^3\Sigma_g^-)$	1.32×10^{12}	0	0	–	–	–
26	$H_2O + O_2(X\,^3\Sigma_g^-) = \dot{O}H + HO_2^{\bullet}$	1.5×10^{15}	0.5	36600	3×10^{14}	0	0
27	$H_2O + O_2(a^1\Delta_g) = \dot{O}H + HO_2^{\bullet}$	1.5×10^{15}	0.5	25209	–	–	–
28	$H_2O + O_2(b\,^1\Sigma_g^+) = \dot{O}H + HO_2^{\bullet}$	1.5×10^{15}	0.5	17616	–	–	–
29	$H_2O + \dot{O}H = H_2 + HO_2^{\bullet}$	7.2×10^{9}	0.43	36100	6.5×10^{11}	0	9400
30	$2\dot{O}H = H^{\bullet} + HO_2^{\bullet}$	1.2×10^{13}	0	20200	2.5×10^{14}	0	950

Table. (Contd.)

No.	Reaction	k_{+q} (cm^3/mol)$^{m-1}$ s^{-1}			k_{-q} (cm^3/mol)$^{m-1}$ s^{-1}		
		A_q	n_q	$E_{a,q}/k$, K	A_q	n_q	$E_{a,q}/k$, K
31	$\dot{O}H + O_2(X^3\Sigma_g^-) = \dot{O}(^3P) + HO_2^\bullet$	1.3×10^{13}	0	28200	5×10^{13}	0	500
32	$\dot{O}H + O_2(a^1\Delta_g) = \dot{O}(^3P) + HO_2^\bullet$	1.3×10^{13}	0	17132	–	–	–
33	$\dot{O}H + O_2(b^1\Sigma_g^+) = \dot{O}(^3P) + HO_2^\bullet$	1.3×10^{13}	0	10111	–	–	–
34	$\dot{O}H + O_2(X^3\Sigma_g^-) = \dot{O}(^1D) + HO_2^\bullet$	–	–	–	$q_X \times 3.96 \times 10^{13}$	0	0
35	$\dot{O}H + O_2(a^1\Delta_g) = \dot{O}(^1D) + HO_2^\bullet$	–	–	–	$q_a \times 3.96 \times 10^{13}$	0	0
36	$\dot{O}H + O_2(b^1\Sigma_g^+) = \dot{O}(^1D) + HO_2^\bullet$	–	–	–	$q_b \times 3.96 \times 10^{13}$	0	0
37	$H_2O_2 + M = 2\dot{O}H + M$	1.2×10^{17}	0	22900	9.1×10^{14}	0	–2650
38	$H^\bullet + H_2O_2 = H_2 + HO_2^\bullet$	1.7×10^{12}	0	1900	6×10^{11}	0	9300
39	$H^\bullet + H_2O_2 = H_2O + \dot{O}H$	5×10^{14}	0	5000	2.4×10^{14}	0	40500
40	$2HO_2^\bullet = H_2O_2 + O_2(X^3\Sigma_g^-)$	1.8×10^{13}	0	500	3×10^{13}	0	21600
41	$2HO_2^\bullet = H_2O_2 + O_2(a^1\Delta_g)$	–	–	–	3×10^{13}	0	10717
42	$2HO_2^\bullet = H_2O_2 + O_2(b^1\Sigma_g^+)$	–	–	–	3×10^{13}	0	4510
43	$HO_2^\bullet + H_2O = H_2O_2 + \dot{O}H$	1.8×10^{13}	0	15100	1×10^{13}	0	910
44	$\dot{O}H + HO_2^\bullet = H_2O_2 + \dot{O}(^3P)$	5.2×10^{10}	0.5	10600	2×10^{13}	0	2950
45	$H_2O + O_2(X^3\Sigma_g^-) = H_2O_2 + \dot{O}(^3P)$	3.4×10^{10}	0.5	44800	8.4×10^{11}	0	2130
46	$H_2O + O_2(a^1\Delta_g) = H_2O_2 + \dot{O}(^3P)$	3.4×10^{10}	0.5	34079	–	–	–
47	$H_2O + O_2(b^1\Sigma_g^+) = H_2O_2 + \dot{O}(^3P)$	3.4×10^{10}	0.5	27195	–	–	–
48	$O_3 + M = \dot{O}(^3P) + O_2(X^3\Sigma_g^-) + M$	4×10^{14}	0	11400	6.9×10^{12}	0	–1050
49	$O_3 + M = \dot{O}(^3P) + O_2(a^1\Delta_g) + M$	4×10^{14}	0	22790	–	–	–
50	$O_3 + M = \dot{O}(^3P) + O_2(b^1\Sigma_g^+) + M$	4×10^{14}	0	30384	–	–	–
51	$O_3 + H^\bullet = \dot{O}H + O_2(X^3\Sigma_g^-)$	2.3×10^{11}	0.75	0	4.4×10^{7}	1.44	38600
52	$O_3 + H^\bullet = \dot{O}H + O_2(a^1\Delta_g)$	–	–	–	4.4×10^{7}	1.44	27209
53	$O_3 + H^\bullet = \dot{O}H + O_2(b^1\Sigma_g^+)$	–	–	–	4.4×10^{7}	1.44	19616
54	$O_3 + \dot{O}(^3P) = 2O_2(X^3\Sigma_g^-)$	1.1×10^{13}	0	2300	1.2×10^{13}	0	50500
55	$O_3 + \dot{O}(^3P) = O_2(X^3\Sigma_g^-) + O_2(a^1\Delta_g)$	–	–	–	1.2×10^{13}	0	39732
56	$O_3 + \dot{O}(^3P) = O_2(X^3\Sigma_g^-) + O_2(b^1\Sigma_g^+)$	–	–	–	1.2×10^{13}	0	32761
57	$O_3 + \dot{O}(^1D) = 2O_2(X^3\Sigma_g^-)$	1.37×10^{13}	0	0	–	–	–
58	$O_3 + \dot{O}(^1D) = O_2(X^3\Sigma_g^-) + O_2(a^1\Delta_g)$	9.1×10^{12}	0	0	–	–	–
59	$O_3 + \dot{O}(^1D) = O_2(X^3\Sigma_g^-) + O_2(b^1\Sigma_g^+)$	4.6×10^{12}	0	0	–	–	–
60	$O_3 + \dot{O}(^1D) = O_2(X^3\Sigma_g^-) + \dot{O}(^3P) + \dot{O}(^3P)$	1.166×10^{14}	0	0	–	–	–

Table. (Contd.)

No.	Reaction	k_{+q} (cm^3/mol)$^{m-1}$ s^{-1}			k_{-q} (cm^3/mol)$^{m-1}$ s^{-1}		
		A_q	n_q	$E_{a,q}/k$, K	A_q	n_q	$E_{a,q}/k$, K
61	$O_3 + \dot{O}H = H\dot{O}_2 + O_2(X\,^3\Sigma_g^-)$	$q_X \times 9.6 \times 10^{11}$	0	1000	9(8)	0	0
62	$O_3 + \dot{O}H = H\dot{O}_2 + O_2(a\,^1\Delta_g)$	$q_a \times 9.6 \times 10^{11}$	0	1000	–	–	–
63	$O_3 + \dot{O}H = H\dot{O}_2 + O_2(b\,^1\Sigma_g^+)$	$q_b \times 9.6 \times 10^{11}$	0	1000	–	–	–
64	$O_3 + H_2 = \dot{O}H + H\dot{O}_2$	6×10^{10}	0	10000	–	–	–
65	$O_3 + H\dot{O}_2 = \dot{O}H + 2O_2(X\,^3\Sigma_g^-)$	$q_X \times 2 \times 10^{10}$	0	1000	–	–	–
66	$O_3 + H\dot{O}_2 = \dot{O}H + O_2(X\,^3\Sigma_g^-) + O_2(a\,^1\Delta_g)$	$q_a \times 2 \times 10^{10}$	0	1000	–	–	–
67	$O_3 + H\dot{O}_2 = \dot{O}H + O_2(X\,^3\Sigma_g^-) + O_2(b\,^1\Sigma_g^+)$	$q_b \times 2 \times 10^{10}$	0	1000	–	–	–
68	$O_3 + O_2(a\,^1\Delta_g) = 2O_2(X\,^3\Sigma_g^-) + \dot{O}(^3P)$	3.13×10^{13}	0	2840	–	–	–
69	$O_3 + O_2(b\,^1\Sigma_g^+) = 2O_2(X\,^3\Sigma_g^-) + \dot{O}(^3P)$	9×10^{12}	0	0	–	–	–
70	$2O_2(a\,^1\Delta_g) = O_2(b\,^1\Sigma_g^+) + O_2(X\,^3\Sigma_g^-)$	4.2×10^{-4}	3.8	–700	–	–	–
71	$O_2(a\,^1\Delta_g) + M = O_2(X\,^3\Sigma_g^-) + M$						
	$M = \dot{O}, \dot{H}$	4.2×10^8	0	0	–	–	–
	$M = O_3$	2.4×10^9	0	0	–	–	–
	$M = O_2$	1.02×10^6	0	0	–	–	–
	$M = H_2$	2.7×10^6	0	0	–	–	–
	$M = H_2O, \dot{O}H, H\dot{O}_2, H_2O_2$	3.36×10^6	0	0	–	–	–
72	$O_2(b\,^1\Delta_g) + M = O_2(a\,^1\Delta_g) + M$						
	$M = \dot{O}, \dot{H}$	4.8×10^{10}	0	0	–	–	–
	$M = O_3$	1.08×10^{13}	0	0	–	–	–
	$M = O_2$	2.76×10^7	0	0	–	–	–
	$M = H_2$	4.92×10^{11}	0	0	–	–	–
	$M = H_2O, \dot{O}H, H\dot{O}_2$	4.02×10^{12}	0	0	–	–	–
	$M = H_2O_2$	6×10^{12}	0	0	–	–	–
73	$\dot{O}(^1D) + O_2(X\,^3\Sigma_g^-) = \dot{O}(^3P) + O_2(a\,^1\Delta_g)$	3.8×10^{12}	0	–67	–	–	–
74	$\dot{O}(^1D) + O_2(X\,^3\Sigma_g^-) = \dot{O}(^3P) + O_2(b\,^1\Sigma_g^+)$	1.54×10^{13}	0	–67	–	–	–
75	$\dot{O}(^1D) + O_2(a\,^1\Delta_g) = \dot{O}(^3P) + O_2(b\,^1\Sigma_g^+)$	3×10^{13}	0	0	–	–	–
76	$\dot{O}(^1D) + M = \dot{O}(^3P) + M$						
	$M = \dot{O}, \dot{H}, O_3, O_2$	1.92×10^{13}	0	–67	–	–	–
	$M = H_2$	3.3×10^{12}	0	0	–	–	–
	$M = H_2O, \dot{O}H, H\dot{O}_2, H_2O_2$	7.2×10^{12}	0	0	–	–	–

Note: q_X, q_a, and q_b represent the multiplicities of degradation of electron states (see the text); k is the Boltzmann constant.

oxygen in the $X^3\Sigma_g^-$, $a^1\Delta_g$, and $b^1\Sigma_g^+$ states, the probability of the formation of $O_2(X^3\Sigma_g^-)$, $O_2(a^1\Delta_g)$, and $O_2(b^1\Sigma_g^+)$ is proportional to the multiplicity of the degradation of the corresponding electron states q_e. For the ground state $X^3\Sigma_g^-$ $q_X = 0.5$, $q_a = 0.33$ for $a^1\Delta_g$, and $q_b = 0.17$ for $b^1\Sigma_g^+$. Using this procedure, we determined the rate constants for the reactions

$$HO_2^{\bullet} + M = \begin{cases} H^{\bullet} + O_2(X^3\Sigma_g^-) + M \\ H^{\bullet} + O_2(a^1\Delta_g) + M \\ H^{\bullet} + O_2(b^1\Sigma_g^+) + M, \end{cases}$$

$$O(^1D) + HO_2^{\bullet} = \begin{cases} \dot{O}H + O_2(X^3\Sigma_g^-) \\ \dot{O}H + O_2(a^1\Delta_g) \\ \dot{O}H + O_2(b^1\Sigma_g^+), \end{cases}$$

$$O_3 + \dot{O}H = \begin{cases} HO_2^{\bullet} + O_2(X^3\Sigma_g^-) \\ HO_2^{\bullet} + O_2(a^1\Delta_g) \\ HO_2^{\bullet} + O_2(b^1\Sigma_g^+), \end{cases}$$

$$O_3 + HO_2^{\bullet} = \begin{cases} \dot{O}H + 2O_2(X^3\Sigma_g^-) \\ \dot{O}H + O_2(X^3\Sigma_g^-) + O_2(a^1\Delta_g) \\ \dot{O}H + O_2(X^3\Sigma_g^-) + O_2(b^1\Sigma_g^+). \end{cases}$$

The pathways of the corresponding reactions are given in the table with certain numbers (nos. 18–20, 34–36, 61–63, and 65–67). The rate constants for the chain propagation reactions involving $O_2(a^1\Delta_g)$ (nos. 10 and 22) were taken from [12], whereas the rate constants for similar reactions involving $O_2(b^1\Sigma_g^+)$ (nos. 11 and 23) were determined by Eqs. (1) and (2) taking into account that the reaction enthalpy ΔH and the activation energy E_a^0 in Eq. (2) correspond to similar parameters for reactions (10) and (22), and $E_e = \Delta E_{ba}$, where ΔE_{ba} is the difference between the energies of the $b^1\Sigma_g^+$ and $a^1\Delta_g$ states of the O_2 molecule ($\Delta E_{ba} = k7593$ K). When determining the rate constants for reactions (46) and (47), in which the excited molecules $O_2(a^1\Delta_g)$ and $O_2(b^1\Sigma_g^+)$ are formed during O_3 molecule dissociation, we assumed that the energy barrier for the reaction increases by a value of the energy of the corresponding excited state E_e ($e = a^1\Delta_g$, $b^1\Sigma_g^+$): $E_a^e = E_a^0 + E_e$, where E_a^0 is the activation energy of the reaction yielding $O_2(X^3\Sigma_g^-)$. For the reactions involving the excited $O(^1D)$ atoms (nos. 8, 13, 25, 57–60, and 73–76), the rate constants were chosen taking into account the results reported in [16, 21, 22]. For the electron–electron (E–E) exchange (reaction (70)) and the electron–translational (E–T) relaxation of the $O_2(a^1\Delta_g)$ and $O_2(b^1\Sigma_g^+)$ states (reactions (71) and (72)), the rate constants were chosen as recommended in [23]. The rate constants for reactions for which the coefficients A_q, n_q, and $E_{a,q}$ are not given in the table were calculated using the principle of detailed equilibrium, whereas the rate constants for the reactions involving nonexcited molecules are taken to be the same as in [15].

FORMULATION OF THE PROBLEM AND MAIN EQUATIONS

Let us analyze the scheme of flow with the stationary shock wave with a slope of the front to the rate vector u_0 of the unperturbed flow $\beta \le 30°$ when the gas rate behind the front remains supersonic [14]. Let us assume thermodynamic equilibrium between the vibrational, rotational, and translational degrees of freedom of the molecules in the mixture and consider that this equilibrium is preserved upon laser-induced transitions and chemical reactions and that the gas is nonviscous and not conducting. Let the homogeneous gas mixture $H_2 + O_2$ moving at a supersonic rate in the interval of length δ before the shock wave is exposed to the radiation with a constant intensity I, whose frequency ν_I is in resonance with the frequency of the given bound–bound electron transition of the O_2 molecule $m(e', v', j', K') \longrightarrow n(e'', v'', j'', K'')$, where $e' = X^3\Sigma_g^-$, $e'' = a^1\Delta_g$ or $b^1\Sigma_g^+$, v' and v'' are the vibrational and j', K' and j'', K'' are the rotational quantum numbers in the e' and e'' states, respectively. Recall that the transitions from the ground state $X^3\Sigma_g^-$ in the $a^1\Delta_g$ and $b^1\Sigma_g^+$ states are permitted only in the magnetic–dipole approximation [24]. Let us consider the electronically excited $O_2(a^1\Delta_g)$ and $O_2(b^1\Sigma_g^+)$ molecules and $O(^1D)$ atoms as separate chemical components with the corresponding enthalpy of formation. In this case, the E–E and E–T processes may be considered as ordinary chemical reactions. Let $\delta \ll L_\nu$, where L_ν is the length of laser radiation absorption. In this case, the system of equations describing the flow both in the zone of radiation action and behind the shock wave front may be represented as follows:

$$u\frac{dN_i}{dx} = Q_{Ii} + Q_{ci} + Q_{si}, \qquad (3)$$

$$u\frac{du}{dx} + \frac{1}{\rho}\frac{dP}{dx} = 0, \quad (4)$$

$$\frac{dH}{dx} + u\frac{du}{dx} = \frac{k_\nu I}{\rho u}. \quad (5)$$

$$H = \sum_{i=1}^{M}\frac{h_{0i}}{\mu}\gamma_i + C_pT;$$

$$C_p = \frac{R}{\mu}\left(\frac{5}{2} + \sum_{i=1}^{S} C_R^i\gamma_i + \sum_{i=1}^{S} C_V^i\gamma_i\right); \quad \mu = \sum_{i=1}^{M}\mu_i\gamma_i;$$

$$C_V^i = \sum_{j=1}^{L}\left(\frac{\theta_{ij}}{T}\right)^2\frac{\exp(\theta_{ij}/T)}{[\exp(\theta_{ij}/T)-1]^{-2}}, \quad \gamma_i = \frac{N_i}{N},$$

$$N = \sum_{i=1}^{M} N_i;$$

$$P = \frac{\rho RT}{\mu};$$

$$Q_{ci} = \sum_{q=1}^{M_1} S_{iq}, \quad S_{iq} = (\alpha_{iq}^- - \alpha_{iq}^+)[R_q^+ - R_q^-],$$

$$R_q^{+(-)} = k_{+(-)q}\prod_{j=1}^{n_q^{+(-)}} N_j^{\alpha_{iq}^{+(-)}};$$

$$Q_{Ii} = l_{iI}W_I\left(\frac{g_n}{g_m}N_m - N_n\right), \quad W_I = \sigma_{mn}I/h\nu_I,$$

$$\sigma_{mn} = \frac{\lambda_{mn}^2}{4\pi b_D}A_{mn}\sqrt{\frac{\ln 2}{\pi}}H(x,a);$$

$$Q_{si} = \sum_q r_{iq}^s\sum_j A_{qj}^s N_j;$$

$$k_\nu = \sigma_{mn}\left(\frac{g_n}{g_m}N_m - N_n\right), \quad N_m = N_1\varphi_m,$$

$$N_n = N_l\varphi_n, \quad l = 2 \text{ or } 3,$$

$$\varphi_m = \frac{g_m B_{v'}}{kT}\frac{\exp(-\theta_1 v'/T)}{1-\exp(-\theta_1/T)}\exp\left(-\frac{E_{j'}}{kT}\right),$$

$$\varphi_n = \frac{g_n B_{v''}}{kT}\frac{\exp(-\theta_1 v''/T)}{1-\exp(-\theta_l/T)}\exp\left(-\frac{E_{j''}}{kT}\right).$$

Here, P, ρ, T, and u are the pressure, density, temperature, and rate of the gas; N_i is the density of the molecules (atoms) of the ith type (i = 1, 2, and 3 correspond to $O_2(X^3\Sigma_g^-)$, $O_2(a^1\Delta_g)$, and $O_2(b^1\Sigma_g^+)$); μ_i is their molecular weight; h_{0i} is the enthalpy of formation of the ith component at T = 298 K; M is the number of the atomic and molecular components in the mixture; S is the number of only molecular components; $C_R^i = 1$ for the components from linear molecules and $C_R^i = 1.5$ for the components from nonlinear molecules; θ_{ij} is the characteristic vibrational temperature of the jth mode for the ith component ($j = 1\ldots L$); M_1 is the number of reactions resulting in the formation (destruction) of the ith component; α_{iq}^+ and α_{iq}^- are the stoichiometric coefficients of the qth reaction; $n_q^{+(-)}$ is the number of the components participating in the direct (+) and reverse (–) reactions, respectively; $k_{+(-)q}$ are the rate constants for these reactions; R is the universal gas constant; h is the Planck constant; k is the Boltzmann constant; l_{iI} and r_{iq}^s represent the number of quanta lost (gained) by the ith component during induced and spontaneous transitions, respectively; N_m and N_n are the number of molecules in the lower and upper states of the absorbed transition $m \longrightarrow n$, respectively; g_m and g_n are the multiplicities of degradation of these states, respectively; λ_{mn} is the wavelength corresponding to the center of the spectral line of the absorbing transition; A_{mn} (A_{qj}^s) is the Einstein coefficient; b_D is the Doppler width of the spectral line of the $m \longrightarrow n$ transition; $H(x, a)$ is the Voigt function; B_v is the rotational constant of the O_2 molecule in the state v ($v' \in m$, $v'' \in n$); and $E_{j'}$ and $E_{j''}$ are the rotational energies of the O_2 molecule in the m and n states, respectively. Their values were calculated taking into account the depletion of the j' level in the $X^3\Sigma_g^-$ state into three components with $j' = K' + 1$, $j' = K'$, and $j' = K' - 1$ [25].

In numerical integration of system (3)–(5), the whole calculation region is divided into two subregions. The first one corresponds to the zone of the action of resonance radiation before the inclined shock wave front (its length $x_0 \le \delta < x_1$), and the second corresponds to the zone of detonation initiation behind the front. Its left boundary is the shock wave front; its right boundary is the cross section x_{eq}, where the equilibrium values of all gas-dynamic parameters and component concentrations of the reacted mixture are attained. The boundary conditions for the system of Eqs. (3)–(5) at $x = x_1$ are the parameters behind the shock wave front (henceforth, denoted with subscript 1), which are determined from the laws of conservation of matter, momentum, and energy assuming that the component concentrations remain unchanged when passing through the front [26]. As in [13, 14], the numerical integration of Eqs. (3)–(5) were carried out using the implicit finite-difference second-order approximation scheme.

LASER-INDUCED O_2 MOLECULE EXCITATION

The analysis was performed for radiation absorption in the center of the spectral line of the transitions $(X^3\Sigma_g^-,\ v',\ j',\ K') \longrightarrow (a^1\Delta_g,\ v'',\ j'',\ K'')$ and $(X^3\Sigma_g^-, v', j', K') \longrightarrow (b^1\Sigma_g^+, v'', j'', K'')$ at $v' = v'' = 0, j' = 9, j'' = K' = K'' = 8$ (the absorption coefficient for both transitions is maximum at these rotational quantum numbers at T_0 = 300 K). The Einstein coefficients A_{mn} for these transitions are 2.58×10^{-4} and 8.5×10^{-2} s^{-1}, respectively. When calculating the Voigt functions $H(x, a)$, we assumed, as in [16], that the coefficients of the collisional broadening of the spectral line are proportional to the gas-kinetic sections of the collisions of the O_2 molecule with the Mth partner (in the radiation zone $M = O_2$ or H_2). At low gas temperatures ($T_0 \approx 300$ K), the rates of chemical reactions in the radiation zone are markedly lower than the rate of the induced transitions and the rate of E–T quenching of the $O_2(a^1\Delta_g)$ and $O_2(b^1\Sigma_g^+)$ states. In this case, a change in the concentrations of the $O_2(a^1\Delta_g)$ and $O_2(b^1\Sigma_g^+)$ molecules is only determined by the time of the induced transitions $\tau_I = W_I^{-1}$, the time of quenching of excited states τ_R, and the exposure time τ_P, which is related to the length δ and the flow rate u_0 according to the equation $\tau_P = \delta/u_0$. Taking into account that the length of the radiation zone δ is markedly shorter than $L_v = k_v^{-1}$ (L_v = 250 nm at $P_0 = 10^3$ Pa, T_0 = 300 K on exposure to radiation with λ_I = 762 nm), the radiation of the flow can be performed by multiple cross-scanning the flow with a rather narrow laser beam (with a radius of 0.2–1 cm).

Figure 1 illustrates the relative concentrations of the excited $O_2(a^1\Delta_g)$ and $O_2(b^1\Sigma_g^+)$ molecules and the gas temperature in the zone of exposure to radiation with a wavelength λ_I of 1.268 μm (the $X^3\Sigma_g^- \longrightarrow a^1\Delta_g$ transition) and 762 nm (the $X^3\Sigma_g^- \longrightarrow b^1\Sigma_g^+$ transition) for two pressures $P_0 = 10^3$ and 5×10^4 Pa at T_0 = 300 K, the Mach number of the unperturbed flow M_0 = 6, and I = 10 kW/cm^2. The concentration of the O_2 ($a^1\Delta_g$) molecules at the end of the radiation zone on excitation of the $a^1\Delta_g$ state (λ_I = 1.268 nm) is noticeably lower than upon excitation of the $b^1\Sigma_g^+$ state (λ_I = 762 nm). This is due to the fact that the rate of the induced transitions W_I on exposure to radiation with λ_I = 762 nm is ~75 times higher at the same value of I. Therefore, there are many O_2 molecules in the $b^1\Sigma_g^+$ state. The collisional quenching of $O_2(b^1\Sigma_g^+)$ (reaction (72)) favors the formation of the $O_2(a^1\Delta_g)$ molecules in the mixture in a concentration that is noticeably (by a factor of 10^2) higher at the end of the radiation zone than the concentration of $O_2(a^1\Delta_g)$ molecules, obtained upon direct excitation of the $a^1\Delta_g$ state by the radiation with λ_I = 1.268 μm, at both P_0 values of 10^3 and 5×10^4 Pa. The $O_2(b^1\Sigma_g^+)$ concentration remains unchanged starting from a certain distance from the beginning of the radiation zone x_s (which depends on the values of I and P_0). This may be attributed to the fact that the rate of induced transitions $b^1\Sigma_g^+$ becomes identical to the quenching rate at $x \geq x_s$.

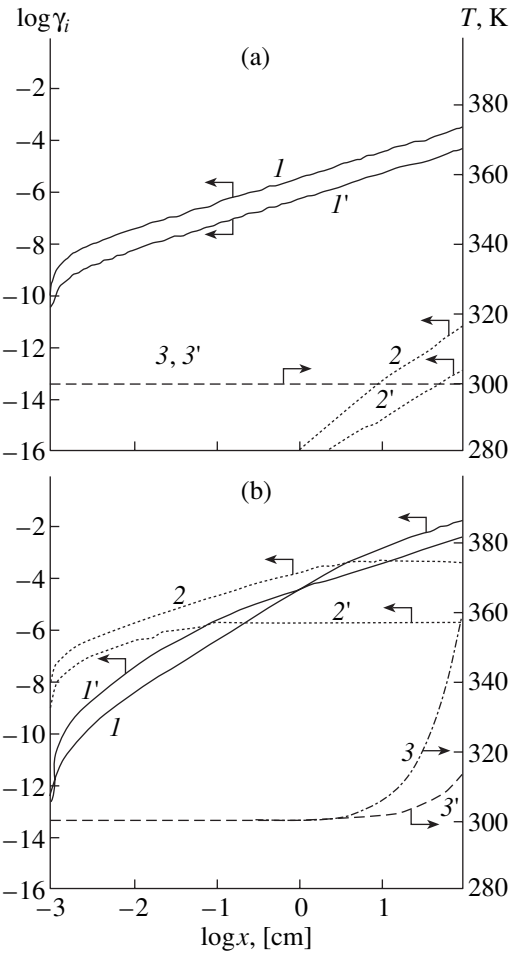

Fig. 1. Variations in the relative concentrations of (*1*, *1'*) $O_2(a^1\Delta_g)$ and (*2*, *2'*) $O_2(b^1\Sigma_g^+)$ and (*3*, *3'*) gas temperature in the $2H_2 + O_2$ mixture in the zone of exposure to radiation with λ_I = (a) 1.268 μm and (b) 762 nm at I = 10 kW/cm^2 for P_0 = (*1*, *2*, *3*) 10^3 and (*1'*, *2'*, *3'*) 5×10^4 Pa.

The $O_2(b^1\Sigma_g^+)$ molecules are also formed at the end of the radiation zone upon excitation of the $a^1\Delta_g$ state because of the E–E exchange $2O_2(a^1\Delta_g) \longrightarrow O_2(b^1\Sigma_g^+) + O_2(X^3\Sigma_g^-)$. However, their concentration is ~10^8 times lower than the $O_2(a^1\Delta_g)$ concentration. It is clear that the

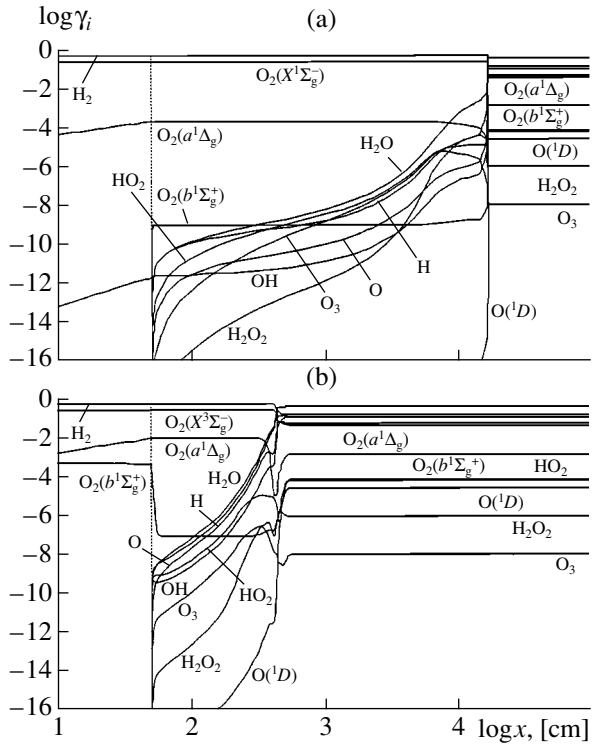

Fig. 2. Variations in the relative concentrations of the components along the flow with $M_0 = 6$ and $\beta = 25°$ upon the exposure of the $2H_2 + O_2$ mixture ($T_0 = 300$ K and $P_0 = 10^3$ Pa) to radiation with λ_I = (a) 1.268 μm and (b) 762 nm, I = 10 kW/cm^2, and $\delta = 0.5$ m.

exposure to radiation with $\lambda_I = 762$ nm provides much more profound excitation of O_2 molecules in the $a^1\Delta_g$ and $b^1\Sigma_g^+$ states.

An increase in the initial pressure of the mixture causes a certain decrease in the values of $\gamma_{O_2(a^1\Delta_g)}$ and $\gamma_{O_2(b^1\Sigma_g^+)}$ at the end of the radiation zone. This may be associated with the fact that an increase in the absorption coefficient k_ν and, consequently, in the rate of induced transitions due to spectral line broadening with an increasing P_0 value becomes nonproportional to N_0 (k_ν is independent of P_0 at $P_0 > 10^5$ Pa). The flow temperature begins to rise on excitation of the O_2 molecules in the $b^1\Sigma_g^+$ state ($\lambda_I = 720$ nm) due to the E–T relaxation of $O_2(b^1\Sigma_g^+)$ (reaction (72)) even at $x = 1$ cm. This temperature increase slows down as the value of P_0 increases because of a decrease in the radiation energy E_s transmitted to one molecule (as follows from the equation $E_s = I\tau_p k_\nu/N_1$ due to a decrease in the k_ν/N_1 ratio). At $P_0 = 10^3$ Pa, $T = 360$ K at the end of the radiation zone ($x = 1$ m) and $T = 313$ K at $P_0 = 5 \times 10^4$ Pa. Note that the temperature at $x = 1$ m would be 443 K at $P_0 = 10^3$ Pa and 333 K at $P_0 = 5 \times 10^4$ Pa if all the radiation energy transformed into thermal energy.

INITIATION OF DETONATION COMBUSTION ON O_2 MOLECULE EXCITATION

The presence of excited molecules $O_2(^1\Delta_g)$ and $O_2(b^1\Sigma_g^+)$ strongly affects the dynamics of mixture ignition by a shock wave. Indeed, even at a low gas temperature behind the shock wave front $T_1 = 646$ K ($M_0 = 6$, $\beta = 25°$) on exposure to radiation with $\lambda_I = 762$ nm at the length $\delta = 50$ cm, the mixture ignites at a distance of 3.9 m from the front even at a very low initial pressure of the gas $P_0 = 10^3$ Pa and low radiation energy transmitted to the gas $E_{in} = I\tau_p = 1.5$ J/cm^2. On exposure to radiation with $\lambda_I = 1.268$ μm, the induction zone length L_{in} is much longer and makes up 167 m. This is clearly seen from Fig. 2, which shows changes in the relative concentrations of the components behind the shock wave front in the case of exposure to radiation with $\lambda_I = 1.268$ μm (a) and 762 nm (b), $I = 10$ kW/cm^2, and $\delta = 0.5$ m at $P_0 = 10^3$ Pa. The vertical dashed line in Fig. 2 indicates the position of the shock wave front. Note here that $L_{in} \sim 10^3$ m in the absence of excitation; that is, ignition does not occur at all. On excitation of the O_2 molecules in the $b^1\Sigma_g^+$ state for the conditions under consideration, the relative concentrations (in %) of the $O_2(a^1\Delta_g)$ and $O_2(b^1\Sigma_g^+)$ molecules at the end of the radiation zone are only 1 and ~0.05%, respectively. However, this concentration of electronically excited O_2 molecules is sufficient for the significant intensification of chain reactions in the $H_2 + O_2$ mixture. It should be noted that it is the excitation of the O_2 molecules rather than the enthalpy of laser radiation that is responsible for the intensification of chain reactions. For example, if all the energy consumed by the gas transformed into its translational degrees of freedom at $\delta = 0.5$ m, $I = 10$ kW/cm^2, and $P_0 = 10^3$ Pa, the temperature before the front would be 379 K and the induction zone length would be ~74 m, which is 20 times higher than the value of L_{in} observed upon O_2 molecule excitation in the $b^1\Sigma_g^+$ state.

Recall that the initiation of combustion in the hydrogen–oxygen mixtures is due to the formation of the $\dot{O}H$ radical and $O^\cdot$ and $H^\cdot$ atoms in the following main reactions: $H_2 + O_2 = 2\dot{O}H$, $\dot{O}H + H_2 = H_2O + H^\cdot$, $H^\cdot + O_2 = \dot{O}H + O^\cdot$, and $O^\cdot + H_2 = \dot{O}H + H^\cdot$. The dissociation of the O_3 molecules ($O_3 + M = O_2 + O^\cdot + M$) in the reaction of $HO_2^\cdot$ with O_2 (reaction (61)) begins to play a noticeable role at low values of T_0. The presence

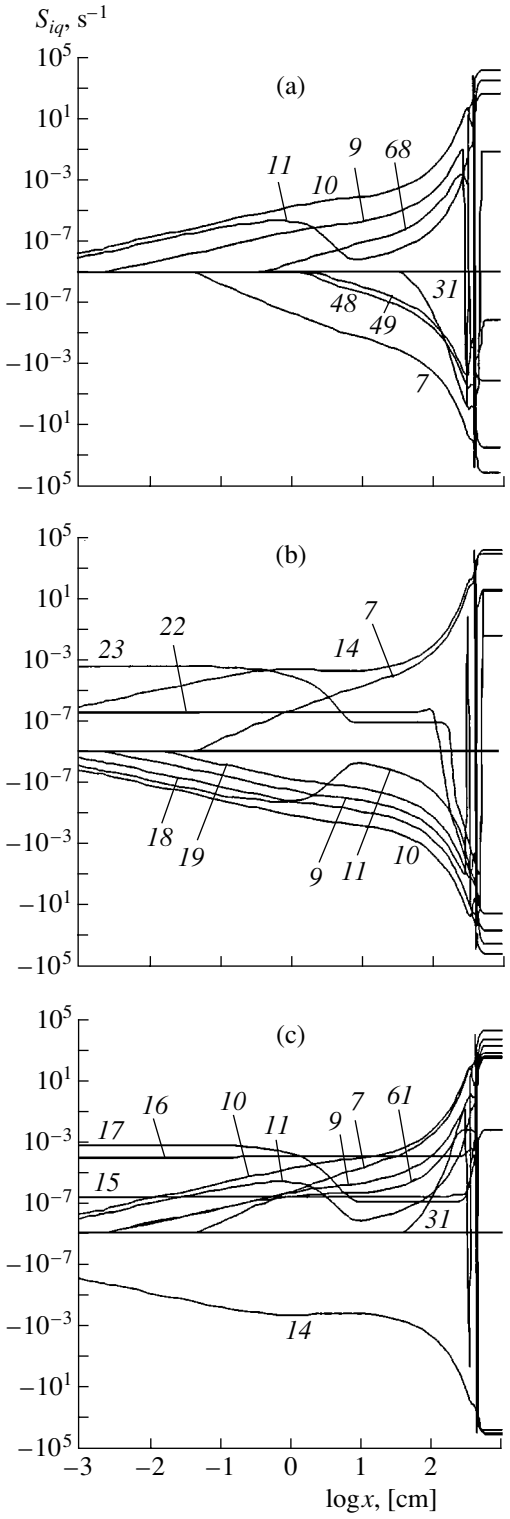

Fig. 3. Variations in the rates S_{iq} for the formation (+) and decomposition (–) of the (a) $O^{\bullet}$ and (b) $H^{\bullet}$ atoms and (c) $\dot{O}H$ radicals behind the shock wave front with $M_0 = 6$, $\beta = 25°$, $T_0 = 300$ K, and $P_0 = 10^3$ Pa upon excitation of $O_2(b\,^1\Sigma_g^+)$ by radiation with $\lambda_I = 762$ nm and $I = 10$ kW/cm^2 at the distance $\delta = 0.5$ m.

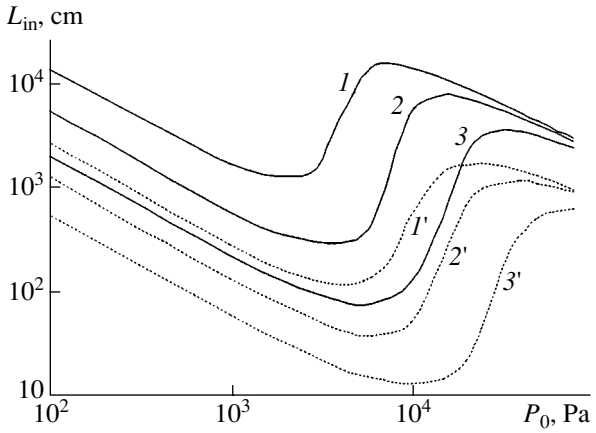

Fig. 4. Length of the induction zone (L_{in}) as a function of the initial pressure during combustion of the $2H_2 + O_2$ mixture ($T_0 = 300$ K) behind the shock wave front with $M_0 = 6$ at $\beta = (1, 2, 3)$ 25° and $(1', 2', 3')$ 30° and different energies of radiation with $\lambda_I = 762$ nm transmitted to the gas $E_{in} = (1, 1')$ 0.5; $(2, 2')$ 1.5; and $(3, 3')$ 3 J/cm^2.

of the excited $O_2(a^1\Delta_g)$ and $O_2(b\,^1\Sigma_g^+)$ molecules in the mixture favors the new pathways of formation of $\dot{O}H$, $O^{\bullet}$, and $H^{\bullet}$ species. These are mainly reactions (10), (11), (16), (17), (22), and (23). Note that reaction (68) involving $O_2(a^1\Delta_g)$ and O_3 molecules significantly contributes to oxygen atom formation at $T_1 < 700$ K. This is illustrated by Fig. 3, which shows how the rates S_{iq} of the formation of $O^{\bullet}$ (a) and $H^{\bullet}$ (b) atoms and $\dot{O}H$ (c) radicals change behind the shock wave front upon exposure to radiation with $\lambda_I = 762$ nm and $E_{in} = 1.5$ J/cm^2. All these processes are very fast. Therefore, the presence of even small amounts of $O_2(a^1\Delta_g)$ and $O_2(b\,^1\Sigma_g^+)$ in the mixture causes a dramatic decrease in the lengths of the induction (L_{in}) and combustion (L_c) zones. The degree of this decrease depends not only on the I value, but also on the mixture parameters behind the shock wave front P_1 and T_1, which are determined by the values of P_0, T_0, M_0, and β. Figure 4 illustrates the dependence of L_{in} on P_0 at $M_0 = 6$, $T_0 = 300$ K, and $\beta = 25°$ and 30° corresponding to $T_1 = 646$ and 791 K at $I = 0$, respectively. There are two regions of P_0 variations for each set of the parameters I (or E_{in}) and β. In one region, L_{in} decreases as P_0 increases, whereas in the other, P_{0b} increases with P_0. The boundary value of P_{0b} separating these regions increases with an increase in L_{in} and T_1. The existence of P_{0b} and an increase in L_{in} at $P_0 > P_{0b}$ may be attributed to the formation of chemically inert H_2O_2 molecules and a decrease in the concentrations of the $O^{\bullet}$ and $H^{\bullet}$ atoms and $\dot{O}H$ radicals [14] at high values of P_0. The higher the I parameter and the $O_2(a^1\Delta_g)$ concentration in the mixture, the higher

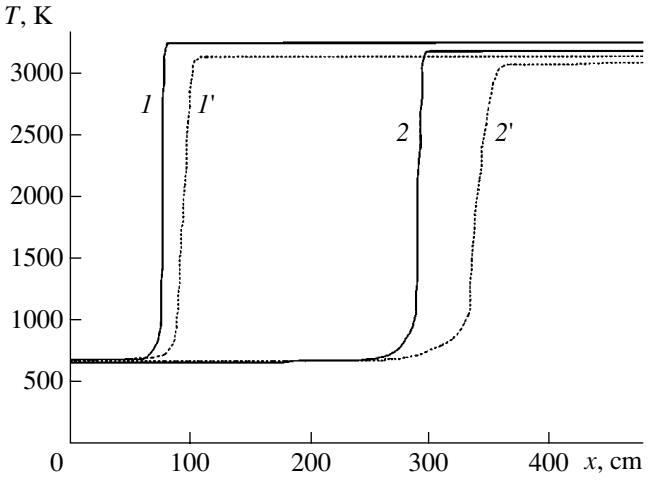

Fig. 5. Variations in the gas temperature behind the shock wave front upon exposure to radiation with λ_I = 762 nm at T_0 = 300 K, M_0 = 6, and β = 25° for E_{in} = (*1*, *1'*) 3 and (*2*, *2'*) 1 J/cm^2 and P_0 = (*1*, *2*) P_{0b} and (*1'*, *2'*) 0.5P_{0b}.

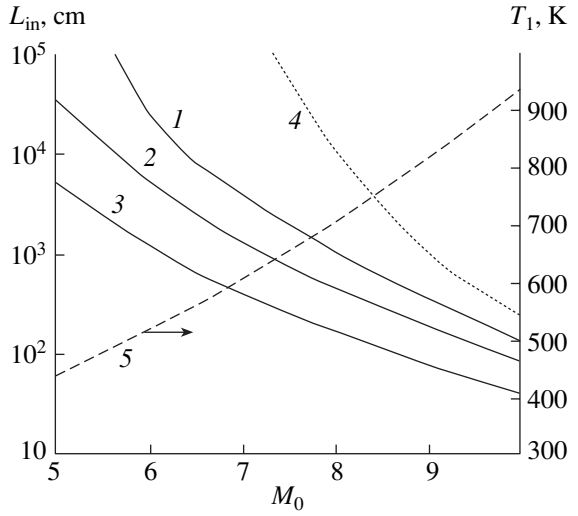

Fig. 6. (*1–4*) The induction zone length L_{in} and (*5*) gas temperature behind the shock wave T_1 vs. M_0 at β = 20°, P_0 = 10^3 Pa, and T_0 = 300 K upon exposure to radiation with λ_I = 762 nm at E_s = (*1*) 0.01, (*2*) 0.03, and (*3*) 0.1 eV/mol and (*4*) in the absence of radiation.

the P_0 values at which these processes start to dominate.

The above findings also suggest that detonation combustion upon exposure of the $H_2 + O_2$ mixture to radiation with λ_I = 762 nm can occur even behind a weak shock wave front (β = 25°, T_1 = 646 K). The value of E_{in} is only ~80 cm at a rather moderate energy transmitted to the gas, L_{in} = 3 J/cm^2 and $P_0 = 6 \times 10^3$ Pa. An increase in the P_{0b} value with an increase in E_{in} favors not only the initiation of detonation at shorter distances from the shock wave front, but also regimes with a higher final temperature of the products T_{eq}. This is demonstrated in Fig. 5, which shows how the gas temperature behind the shock wave front (M_0 = 6, T_0 = 300 K, β = 25°) changes at $P_0 = P_{0b}$ and $P_0 = 0.5P_{0b}$ for two different values of E_{in}. For example, for the shock wave with M_0 = 6, β = 25°, and $P_0 = P_{0b}$, the value of T_{eq} increases by 65 K with a simultaneous threefold decrease in E_{in} as E_{in} increases from 1 to 3 J/cm^2. Note that the value of E_{in} = 3 J/cm^2 at $P_0 = P_{0b} = 6 \times 10^3$ Pa corresponds to a rather low radiation energy with λ_I = 762 nm consumed by the gas per one O_2 molecule $E_s = 5.8 \times 10^{-2}$ eV/molecule. At E_{in} = 1 J/cm^2 and the corresponding value of $P_{0b} = 4 \times 10^3$ Pa, we have $E_s = 2.5 \times 10^{-2}$ eV/molecule.

Another important factor largely determining the induction zone length behind the shock wave is the Mach number of the unperturbed flow M_0. Figure 6 demonstrates how the L_{in} parameter changes with the value of M_0 when the mixture is irradiated with λ_I = 762 nm at different energy consumed by one O_2 molecule E_s = 0.01, 0.03, and 0.1 eV/molecule. For comparison, Fig. 6 also shows how L_{in} changes with M_0 in the absence of radiation. An increase in the value of M_0 causes a decrease in the L_{in} parameter at all energies E_s mainly due to a temperature increase behind the shock wave front. However, even at a low temperature behind the front (T_1 ~ 700 K) and the low value E_s = 0.1 eV/molecule, detonation may be initiated even at a distance of 1.7 m from the front. In the absence of radiation, this distance would be ~115 m. The action of radiation with λ_I = 762 nm allows one to decrease the value of L_{in} several times even at relatively high gas temperature behind the front T_1 ~ 900 K (M_0 = 10, β = 20°) when chain reactions occur at a rather high rate in the mixtures lacking electronically excited O_2 molecules.

CONCLUSION

Molecular oxygen excitation by resonance laser radiation in the $O_2(b^1\Sigma_g^+)$ and $O_2(a^1\Delta_g)$ states makes it possible to initiate the detonation combustion in the supersonic flow of the $H_2 + O_2$ mixture behind the front of relatively weak shock waves when the gas temperature is less than 700 K even at the low density of the radiation energy transmitted to the gas E_{in} ~ 0.5 J/cm^2 due to the new pathways of formation of the active $H^{\bullet}$ and $O^{\bullet}$ atoms and $\dot{O}H$ radicals acting as chain carriers. The excitation of the O_2 molecules in the $b^1\Sigma_g^+$ state by laser radiation with wavelength λ_I = 762 nm has a much stronger effect on the kinetics of detonation initiation compared to $O_2(a^1\Delta_g)$ excitation by radiation with λ_I = 1.268 μm. This is due to the fact that substantially higher (by a factor of ~75) intensities of acting radiation are required to provide the same energy consumed by one O_2 molecule. An increase in the radiation energy transmitted to the gas makes it possible to both initiate

detonation at low gas temperatures at shorter distances from the shock wave front and conduct detonation combustion with a higher final temperature of the products. Taking into account that O_2 molecule excitation by resonance laser radiation intensifies chain reactions, this method of detonation initiation also seems to be quite efficient for combustible mixtures based on hydrocarbons.

ACKNOWLEDGMENTS

The work was supported by the Russian Foundation for Basic Research (project nos. 02-01-00703 and 02-02-16915).

REFERENCES

1. Jaggers, H.C. and von Engel, A., *Combust. Flame*, 1971, vol. 16, no. 3, p. 275.
2. Basevich, V.I. and Belyaev, A.A., *Kinet. Katal.*, 1966, vol. 7, no. 4, p. 487.
3. *Advanced Combustion Methods*, Weinberg, F.J., Ed., London: Academic, 1986.
4. Arnold, S.T., Viggiano, A.A., and Morris, R.A., *J. Phys. Chem.*, 1997, vol. 101, no. 49, p. 9351.
5. Kof, L.M., Strarikovskaia, S.M., and Strarikovskii, A.Yu., *12th Int. Conf. on Gas Discharge and Its Applications, Greifswaild*, 1997, vol. 1, p. 380.
6. Seleznev, A.A., Aleinikov, A.Yu., and Yaroshenko, V.V., *Khim. Fiz.*, 1999, vol. 18, no. 5, p. 65.
7. Tanoff, M.A., Smooke, M.D., Teets, R.E., and Sell, J.A., *Combust. Flame*, 1995, vol. 103, no. 4, p. 253.
8. Ma, J.X., Alexander, D.R., and Poulain, D.E., *Combust. Flame*, 1998, vol. 112, no. 4, p. 492.
9. Morsy, M.H., Ko, Y.S., and Chung, S.H., *Combust. Flame*, 1999, vol. 119, no. 4, p. 473.
10. Brown, R.C., *Combust. Flame*, 1985, vol. 62, no. 1, p. 1.
11. Starik, A.M. and Dautov, N.G., *Dokl. Ross. Akad. Nauk*, 1994, vol. 336, no. 5, p. 617.
12. Basevich, V.Ya. and Belyaev, A.A., *Khim. Fiz.*, 1989, vol. 8, no. 8, p. 1124.
13. Starik, A.M. and Dautov, N.G., *Dokl. Ross. Akad. Nauk*, 1996, vol. 350, no. 6, p. 757.
14. Starik, A.M. and Titova, N.S., *Zh. Tekh. Fiz.*, 2001, vol. 71, no. 8, p. 1.
15. Starik, A.M. and Titiova, N.S., *High-Speed Deflagration and Detonation: Fundamentals and Control.*, Roy, G., Frolov, S., Netzer, D., and Borisov, A.M., Eds. Moscow: Elex-KM, 2001, p. 63.
16. Starik, A.M. and Taranov, O.V., *Khim. Fiz.*, 1999, vol. 18, no. 3, p. 15.
17. Dougherty, E.P. and Rabitz, H., *J. Chem. Phys.*, 1980, vol. 72, no. 12, p. 6571.
18. Rusanov, V.D. and Fridman, A.A., *Fizika khimicheski aktivnoi plazmy* (Physics of a Chemically Active Plasma), Moscow: Nauka, 1984.
19. Lashin, A.M. and Starikovskii, A.Yu., *Nonequilibrium Processes and Their Applications, III Int. School–Seminar*, Minsk, 1996, p. 95.
20. Zakharov, A.I., Klopovskii, K.S., Osipov, A.P., *et al.*, *Fiz. Plazmy*, 1988, vol. 14, no. 3, p. 327.
21. Atkinson, R., Baulch, D.L., Cox, R.A., Hampson, R.F., *et al.*, *J. Phys. Chem. Ref. Data*, 1992, vol. 21, no. 6, p. 1125.
22. Biryukov, A.S., Reshetnyak, S.A., Shelepin, L.A., *Trudy FIAN* (Collected Works of Lebedev Physics Institute), 1979, vol. 107, p. 179.
23. Kulagin, Yu.A., Shelepin, L.A., and Yarygina, V.I., *Trudy FIAN* (Collected Works of Lebedev Physics Institute), 1994, vol. 212, p. 166.
24. Amiot, C. and Verges, J., *Can. J. Phys.*, 1981, vol. 59, no. 8, p. 1391.
25. Landau, L.D. and Lifshits, E.M., *Kvantovaya mekhanika: Nerelyativistskaya teoriya* (Quantum Mechanics: Nonrelativistic Theory), Moscow: Nauka, 1974, vol. 3.
26. Starik, A.M. and Titova, N.S., *Fiz. Goreniya Vzryva*, 2000, vol. 36, no. 3, p. 31.